Flexible Control of Multimaterial Tetrahedral Mesh Properties by Using Multiresolution Techniques

Hiroaki Date, So Noguchi, Masahiko Onosato, and Satoshi Kanai

Graduate School of Information Science and Technology, Hokkaido University, Sapporo 060-0814, Japan

This paper describes a method for flexibly controlling the properties of a given multimaterial tetrahedral mesh for finite-element analysis. Our method is based on multiresolution techniques. A given mesh is first subdivided and then simplified so that the resulting mesh satisfies the user-specified thresholds for mesh properties (element size, shape, valence, and geometric tolerance). Once the simplification is completed, mesh resolution and density can be modified quickly by using level of detail.

Index Terms—**Finite-element analysis, mesh generation, multimaterial, multiresolution, tetrahedral mesh.**

I. Introduction

THE generation of high-quality mesh is a key technology for improving the efficiency and shortening the time of finite-element analysis. In particular, flexible control of certain mesh properties, such as element size, element shape, and valence of nodes is required for performing an efficient and accurate analysis. We have developed a method for improving the quality and controlling certain properties of given triangular meshes [1]. This method is based on the multiresolution technique of mesh models (i.e., mesh subdivision, mesh simplification, and level of detail (LOD).

This paper describes an extension of our previous method [1] of multimaterial tetrahedral meshes for electromagnetic (EM) analysis, and shows the effectiveness of a multiresolution-based method. The central feature of the proposed method is flexible and robust control of the properties (element size, element shape quality, valence of node, and geometric tolerance) of a given tetrahedral mesh use thresholds for each property. Through mesh subdivision and simplification, high-quality meshes with controlled size, quality, valence, and tolerance are generated from a given mesh. Furthermore, by using the LOD technique, meshes with different resolutions can be obtained quickly. Therefore, the multiresolution mesh with good properties is useful for the adaptive finite-element method (FEM) and the multigrid method.

For tetrahedral mesh generation, the Delaunay method, octree method, and advancing front method [2] are widely used and implemented in many commercial finite-element meshers. Recent extended approaches, for example, in [3], can create well-shaped tetrahedral meshes robustly. The meshes generated by these methods can be used as inputs of our method. The methods for simplifying tetrahedral meshes have also been proposed [4], [5]. However, explicit mesh property control was not considered, and applicableness to the analysis was not shown. This paper provides a new strategy for mesh property control and a simple scheme of mesh simplification considering the application of simplified meshes to the finite-element analysis, and shows the effectiveness of mesh property control based on mesh simplification to the analysis.

Manuscript received October 07, 2008. Current version published February 19, 2009. Corresponding author: H. Date (e-mail: hdate@ssi.ist.hokudai.ac.jp).
Digital Object Identifier 10.1109/TMAG.2009.2012623

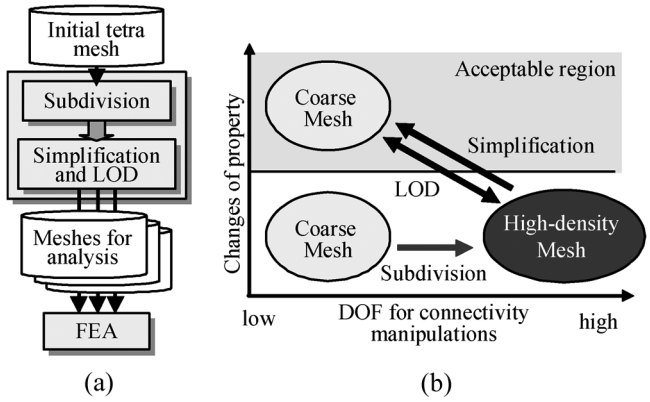

Fig. 1. Overview of our method. (a) Mesh generation procedure for finite-element analysis. (b) Mesh processing strategy.

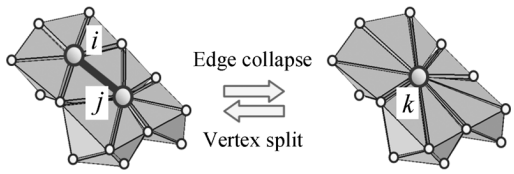

Fig. 2. Edge collapse and vertex (node) split.

II. Basic Concept and Overview

The basic strategy for controlling the mesh properties is to manage them via simplification of a high-density mesh. Therefore, a given mesh is first subdivided in order to obtain enough degrees of freedom for property control in the simplification. Then, the resulting mesh is simplified as shown in Fig. 1. In our method, four mesh properties can be controlled by using thresholds for each property. They are geometric tolerance in the simplification τ_{TL}, upper limit of element size (target size) τ_{SZ}, lower limit of stretch τ_{ST}, and the upper limit of the valence of node τ_{VL}. As a result, the mesh satisfying them can be obtained.

In our method, we subdivide the mesh simply by inserting midpoints for all edges exceeding a certain length, which is experimentally determined as half of the target size. In the simplification step, an edge collapse operation [6] (EC: $(i, j) \rightarrow k$) as shown in Fig. 2 is adopted. The EC collapses an edge to a single node, and its inverse operation is known as the vertex split.

III. Metrics of Mesh Properties

Before describing the detailed algorithm for simplification, we will show the metrics for the evaluation of mesh properties.

A. Geometric Errors in Simplification

The geometric error of the model surface and boundary between the materials caused by applying an edge collapse $(i,j) \rightarrow k$ is evaluated by using the method of quadric error metrics [7]. This error represents the sum of squared distances between the new node position and the planes, which are defined by triangular faces connected to vertices. The error $e_{ij}(k)$ for an edge (i,j) can be written as follows:

$$e_{ij}(k) = \mathbf{p}_k^T \mathbf{A}_{ij} \mathbf{p}_k + 2\mathbf{B}_{ij}\mathbf{p}_k + C_{ij} \tag{1}$$

where $\mathbf{A}_{ij} = \mathbf{A}_i + \mathbf{A}_j$, $\mathbf{B}_{ij} = \mathbf{B}_i + \mathbf{B}_j$, $C_{ij} = C_i + C_j$, $\mathbf{A}_i = \sum_{f \in f^*(i)} \mathbf{n}_f \mathbf{n}_f^T$, $\mathbf{B}_i = -\sum_{f \in f^*(i)} (\mathbf{n}_f^T \mathbf{p}_i)\mathbf{n}_f^T$, and $C_i = \sum_{f \in f^*(i)} (\mathbf{n}_f^T \mathbf{p}_i)^2$, the $\mathbf{n}_f$ and $\mathbf{p}_k$ shows the unit normal vector of the triangular element f and position of node k, and $f^*(i)$ indicates the set of triangular elements on the model surface and material boundary connected to node i.

B. Element Size

The size s_t of a tetrahedral element t is defined as the longest edge (side) length of the tetrahedron $s_t = \max_{e \in e^*(t)} l_e$, where l_e is the length of the edge e of the tetrahedron, and $e^*(t)$ is a set of the edges of tetrahedron t.

C. Element Shape Quality

The element shape quality is evaluated by using stretch (the radius ratio [2]). Stretch is defined by the normalized ratio of the radius of the inscribed sphere and the radius of the circumscribed sphere of the tetrahedron, and is calculated by

$$d_t = 6\sqrt{6} v_t / s_t a_t \tag{2}$$

where v_t and a_t are the volume and the surface area of tetrahedron t. The value of stretch is 1 for a regular tetrahedron, and decreases gradually for distorted tetrahedrons. The value of stretch becomes zero for the degenerated tetrahedron.

IV. Mesh Simplification for Property Control

A. Simplification Method

1) Algorithm: The mesh simplification algorithm is shown in Fig. 3. First, for all edges, new node positions for EC are calculated (step 1). Then, all edges are checked for whether EC can be applied or not (step 2). The edges satisfying the user-specified thresholds are identified as valid edges. If there are no valid edges, the algorithm terminates. Next, for each valid edge, the priority index for determining the order of EC operations is calculated (step 3). Finally, EC is applied to the edge with the largest priority index, then returns to step 1 (step 4).

2) New Node Position Calculation: The midpoint and endpoints of each edge are adopted as candidates for the new node position. For edges incident to inner nodes and those on the boundary/surface of the materials, the new position is set to that of the nodes on the material's boundary/surface for the preservation of their geometry.

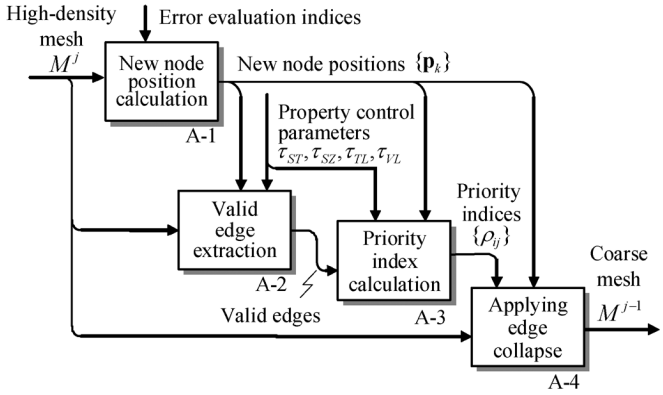

Fig. 3. Mesh simplification algorithm.

3) Valid Edge Extraction: In step 2, all edges are checked for whether the local mesh near the edge satisfies the user-specified mesh property control parameters after the edge collapse operation. Candidates for the new position are progressively tested, and if a candidate passes the test, then it is adopted as the new node position. The edges are identified as valid when they satisfy the following conditions:

- geometric tolerance $e_{ij}(k) \leq \tau_{TL}$;
- the lower limit of the stretch $\forall t \in t^*(k)$; $d_t \geq \tau_{ST}$;
- the upper limit of the element size $\forall t \in t^*(k)$; $s_t \leq \tau_{SZ}$;
- the upper limit of the valence

$$|v^*(i)| + |v^*(j)| - (|f^*(i,j)| + 2) \leq \tau_{VL}$$

where $v^*(i)$, $t^*(i)$, and $f^*(i,j)$ show a set of neighboring nodes of the node i, a set of the tetrahedrons connected to the i, and a set of triangular elements connected to the edge (i,j). Note that evaluations for $t^*(k)$ can be performed for the elements connected to a new node k in EC, which are created temporarily by using the new positions of k.

Moreover, the inner edges connecting the nodes on the surfaces of a material become invalid edges for preserving the the model topology.

4) Priority Index Calculation: The priority index, which shows the priority of edge collapse applications, is calculated for each valid edge. Several definitions of the priority index can be considered, and they determine the characteristics of the resulting mesh in the simplification. We defined the priority index ρ_{ij} for the valid edge by the degree of element shape-quality improvement weighted by the ratio between the current and target (user-specified) element sizes. It is written by

$$\rho_{ij} = \Delta s_{ij}(k) \Delta d_{ij}(k) \tag{3}$$

where $\Delta s_{ij}(k)$ shows the ratio between the thresholds (target) for element size and average size of the elements connected to the new node k: $\Delta s_{ij}(k) = \tau_{SZ}|t^*(k)| / \sum_{t \in t^*(k)} s_t$. The $\Delta d_{ij}(k)$ shows the degree of the element-shape-quality improvement before and after the EC $\Delta d_{ij}(k) = |t^*(i) \cup t^*(k)| \sum_{t \in t^*(k)} d_t / (|t^*(k)| \sum_{t \in t^*(i) \cup t^*(j)} d_t)$. If we apply the edge collapse to the edge (i,j) with larger ρ_{ij}, then we can obtain a local mesh with higher quality and closer-sized elements

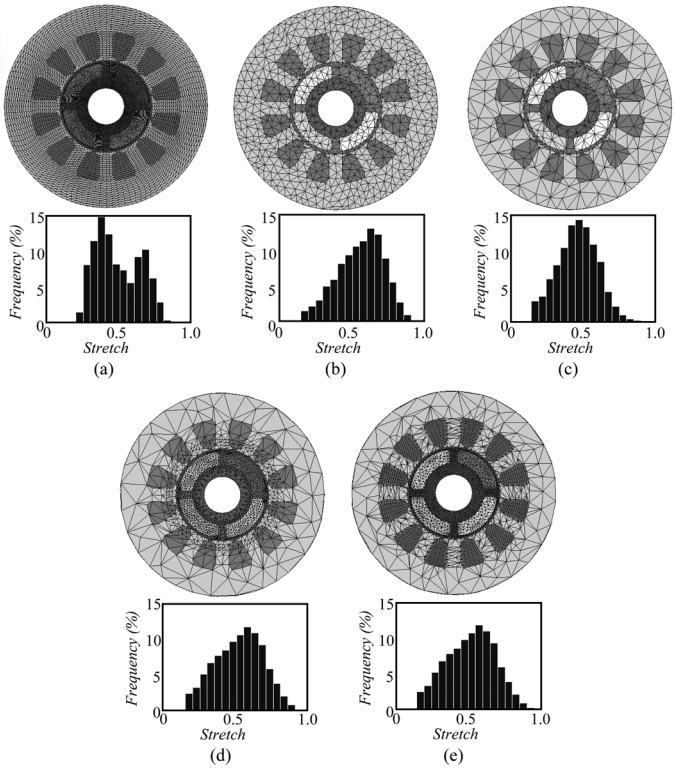

Fig. 4. Resulting meshes. Upper figures show the meshes and lower figures show the stretch distributions. (a) Original multimaterial tetrahedral mesh of motor. (b) and (c) Uniformly simplified meshes. (d) Locally dense mesh obtained by distance-based size settings. (e) Locally dense mesh obtained from different size settings by materials.

TABLE I
PROPERTIES OF RESULTING MESHES

Mesh	Fig.4(a)	Fig.4(b)	Fig.4(c)	Fig.4(d)	Fig.4(e)
#nodes	*41k*	*1930*	*972*	*5935*	*14107*
#edges	*263k*	*9764*	*4706*	*35501*	*88055*
#elements	*210k*	*4075*	*2807*	*26467*	*68838*
Ave. stretch	*0.48*	*0.55*	*0.46*	*0.51*	*0.49*
Min stretch	*0.18*	*0.15(0.15)*	*0.15(0.15)*	*0.15(0.15)*	*0.15(0.15)*
Max valence	*20*	*25(25)*	*25(25)*	*25(25)*	*25(25)*
Max size	*2.20*	*3.00(3)*	*6.00(6)*	*7.99(8)*	*7.99(8)*

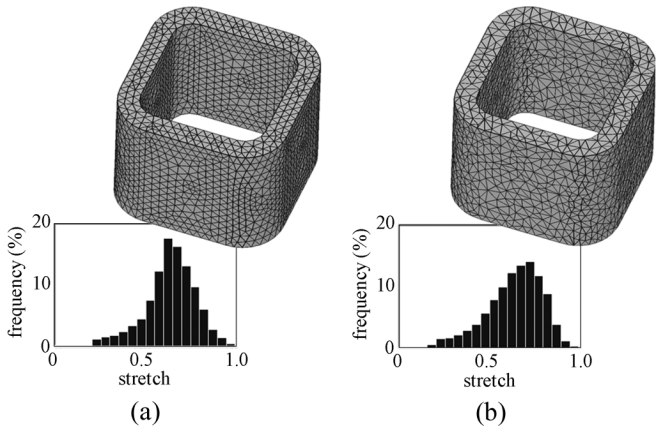

Fig. 5. Comparison of the meshes. (a) Mesh generated by the Delaunay method and its stretch distribution. (b) A mesh generated by out method and its stretch distribution.

to the target in the coarse mesh. Therefore, the edge collapse is applied to the edge with the largest priority index ρ_{ij}.

B. LOD

Meshes with different resolutions can be obtained by quickly using the LOD technique after simplification. Two removed nodes i, j, a generated new node k, and removed tetrahedrons connecting the edge (i, j) are stored as LOD information in each EC application $(i, j) \rightarrow k$. The vertex split is achieved by replacing node k into i, j, inserting removed tetrahedrons, and by modifying the node connectivity of tetrahedrons connected to the node k, and vice-versa in EC. These operations can be performed rapidly; therefore, swift control of a number of elements can be realized after the simplification.

C. Local Property Control

In our method, the thresholds for mesh properties can be assigned into each edge. Therefore, local property control in simplification can be achieved using different thresholds at local regions. In our implementation, three methods for element size control are realized: uniform sizing, region-based sizing, and material-based sizing. Examples are shown in chapter V.

V. EXPERIMENTAL RESULTS AND APPLICATIONS

A. Resulting Meshes

Fig. 4 shows the resulting meshes of our simplification method for a PM motor model consisting of three materials and their stretch distributions. The initial mesh shown in Fig. 4(a) was created by the tetrahedralization of a hexahedral mesh. Fig. 4(b) and (c) is the result of uniform-size simplification. Fig. 4(d) shows the mesh obtained by different size settings according to the distance from the origin (center of rotor). The mesh in Fig. 4(e) was generated from different size settings by materials. In the resulting meshes, the surface of the mesh and boundary shapes between materials were preserved according to user-specified tolerance, and flexible density control could be achieved through simplification.

Table I summarizes evaluations of the mesh properties. The values in brackets denote the user-specified property control parameters. The results show that our approach could generate a mesh that has controlled limits of face size, stretch, and valence by specifying the property control parameters.

The computation time of the simplification from Fig. 4(a)–(c) was about 40 s by using a PC (P-Core2 Duo 3.0 GHz). The processing times for changing the number of tetrahedral elements by using the LOD were less than 1 s in all examples [e.g., Fig. 4(a)–(c)]. This means that our method can efficiently generate meshes that are suitable for limited computer resources for analysis.

B. Comparison

Fig. 5 shows comparisons between the meshes resulting from our approach and commercial software, which adopt Delaunay's method [2]. The high-density mesh with 105 k tetrahedral and 22-k nodes was also generated by the Delaunay method as an input of our method, and then simplification was

TABLE II
COMPARISON OF MESH PROPERTIES

	#nodes	*#edges*	*#elements*	*Ave. stretch*	*Min. stretch*	*Max. valence*	*Max. size*
Fig. 5(a)	*3642*	*20374*	*14052*	*0.63*	*0.19*	*24*	*5.55*
Fig. 5(b)	*3642*	*21207*	*15408*	*0.64*	*0.19*	*25(25)*	*5.37(6)*

applied to it. The comparison of the mesh properties is summarized in Table II. Comparing our mesh with the one obtained by the Delaunay method, although structural regularity is not seen in our mesh, the element shape quality of our mesh is similar to the output of the Delaunay method.

C. Application to Finite-Element Analysis

The cogging torque of the PM motor was evaluated through finite-element analysis by using the meshes shown in Figs. 4(a) and 6(a). The high-density mesh was generated by a uniform subdivision of Fig. 4(a), and the locally dense simplified mesh was generated by our method. The torque and mechanical angle are shown in Fig. 6(b). Compared with the result of the high-density mesh, the simplified mesh provided higher accuracy of analysis than that of the mesh shown in Fig. 4(a), and the number of elements of the simplified mesh were smaller than that of the original mesh. This means that the air and magnetic regions were meshed by better-quality elements and sizes by using our method.

VI. CONCLUSION

In this paper, a flexible property control method for multimaterial tetrahedral meshes based on multiresolution techniques was proposed. The basic approach was to manage mesh properties in mesh simplification of high-density mesh by using new priority indices and EC application rules considering mesh properties for analysis. Geometric tolerance, element size, stretch, and valence of nodes could be controlled by using the thresholds for each property. Once mesh simplification is performed, the mesh with the desired numbers of nodes could be obtained quickly by using LOD. Finally, the effectiveness of our approach was shown via evaluations of mesh properties, a comparison with the traditional meshing method, and the finite-element analysis. These results showed that our method could generate meshes which have a similar quality to the traditional meshing method, and improve the accuracy of analysis by using the mesh with a smaller number of elements.

Our future works are as follows: fast local density control by LOD using nodes hierarchy [8] and its application to the adaptive FEM, and higher-quality mesh generation considering the regularity of the mesh connectivity and symmetries.

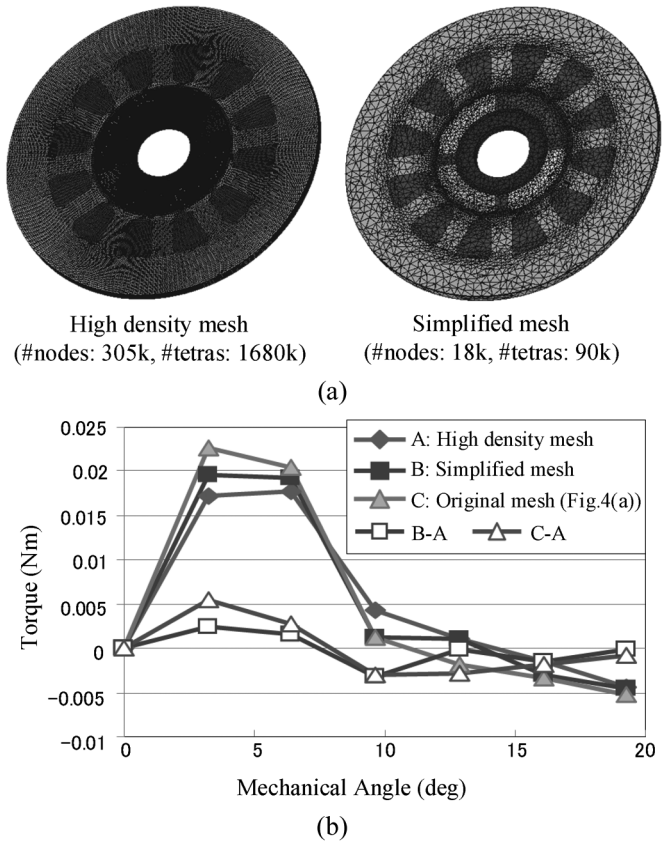

Fig. 6. Results of finite-element analysis by using our meshes. (a) The meshes used in analysis. (b) Cogging torque.

REFERENCES

[1] H. Date, S. Kanai, T. Kishinami, and I. Nishigaki, "High quality and property controlled finite element mesh generation from triangular meshes using multiresolution technique," *ASME J. Comput. Inf. Sci. Eng.*, vol. 5, no. 4, pp. 266–276, 2005.

[2] B. H. V. Topping, J. Muylle, P. Iványi, R. Putanowicz, and B. Cheng, *Finite Element Mesh Generation*. Stirling, U.K.: Saxe-Couburg Publications, 2004.

[3] P. Alliez, D. C. Steiner, M. Yvinec, and M. Desbrun, "Variational tetrahedral meshing," *ACM Trans. Graph.*, vol. 24, pp. 617–625, 2005.

[4] O. G. Staadt and M. H. Gross, "Progressive tetrahedralizations," in *Proc. IEEE Visualization*, 1998, pp. 397–402.

[5] B. Cutler, J. Dorsey, and L. McMillan, "Simplification and improvement of tetrahedral models for simulation," in *Proc. Eurographics Symp. Geometry Processing*, 2004, pp. 95–104.

[6] H. Hoppe, "Progressive meshes," in *Proc. SIGGRAPH*, 1996, pp. 99–108.

[7] M. Garland and P. S. Heckbert, "Surface simplification using quadric error metrics," in *Proc. SIGGRAPH*, 1997, pp. 209–216.

[8] H. Date, S. Kanai, T. Kishinami, and I. Nishigaki, "Mesh simplification and adaptive LOD for finite element mesh generation," *Int. J. CAD/CAM*, vol. 6, no. 1, pp. 69–75, 2006.